

Loss of cochlear HCO₃⁻ secretion causes deafness via endolymphatic acidification and inhibition of Ca²⁺ reabsorption in a Pendred syndrome mouse model

Philine Wangemann, Kazuhiro Nakaya, Tao Wu, Rajanikanth J. Maganti, Erin M. Itza, Joel D. Sanneman, Donald G. Harbidge, Sara Billings, and Daniel C. Marcus

Anatomy and Physiology Department, Kansas State University, Manhattan, Kansas

Submitted 11 December 2006; accepted in final form 31 January 2007

Wangemann P, Nakaya K, Wu T, Maganti RJ, Itza EM, Sanneman JD, Harbidge DG, Billings S, Marcus DC. Loss of cochlear HCO₃⁻ secretion causes deafness via endolymphatic acidification and inhibition of Ca²⁺ reabsorption in a Pendred syndrome mouse model. *Am J Physiol Renal Physiol* 292: F1345–F1353, 2007. First published February 13, 2007; doi:10.1152/ajprenal.00487.2006.— Pendred syndrome, characterized by childhood deafness and postpuberty goiter, is caused by mutations of *SLC26A4*, which codes for the anion exchanger pendrin. The goal of the present study was to determine how loss of pendrin leads to hair cell degeneration and deafness. We evaluated pendrin function by ratiometric microfluorometry, hearing by auditory brain stem recordings, and expression of K⁺ and Ca²⁺ channels by confocal immunohistochemistry. Cochlear pH and Ca²⁺ concentrations and endocochlear potential (EP) were measured with double-barreled ion-selective microelectrodes. Pendrin in the cochlea was characterized as a formate-permeable and DIDS-sensitive anion exchanger that is likely to mediate HCO₃⁻ secretion into endolymph. Hence endolymph in *Slc26a4*^{+/-} mice was more alkaline than perilymph, and the loss of pendrin in *Slc26a4*^{-/-} mice led to an acidification of endolymph. The stria vascularis of *Slc26a4*^{-/-} mice expressed the K⁺ channel *Kcnj10* and generated a small endocochlear potential before the normal onset of hearing at postnatal day 12. This small potential and the expression of *Kcnj10* were lost during further development, and *Slc26a4*^{-/-} mice did not acquire hearing. Endolymphatic acidification may be responsible for inhibition of Ca²⁺ reabsorption from endolymph via the acid-sensitive epithelial Ca²⁺ channels *Trpv5* and *Trpv6*. Hence the endolymphatic Ca²⁺ concentration was found elevated in *Slc26a4*^{-/-} mice. This elevation may inhibit sensory transduction necessary for hearing and promote the degeneration of the sensory hair cells. Degeneration of the hair cells closes a window of opportunity to restore the normal development of hearing in *Slc26a4*^{-/-} mice and possibly human patients suffering from Pendred syndrome.

pendrin; stria vascularis; *Slc26a4*; *Kcnj10*; *Trpv5*

PENDRED SYNDROME IS an autosomal-recessive disorder caused by mutations of the *SLC26A4* gene that codes for the protein pendrin (10). Childhood deafness, postpuberty goiter, and an enlarged endolymphatic duct are the hallmarks of Pendred syndrome (12, 28, 30, 32). Although deafness is generally profound, it is variable and sometimes late in onset (6, 41). Studies of Pendred syndrome have recently been facilitated by the development of an animal model (*Slc26a4*^{-/-} mice) and pendrin-specific polyclonal antibodies (9, 33). Expression has been found in the inner ear and thyroid gland consistent with

the clinical manifestations of deafness and goiter (10, 11, 32, 44). In addition, pendrin expression has been found in the kidney (33), mammary gland (31), uterus (39), testes (20), and placenta (2). No expression was found in fetal or adult brain, consistent with a peripheral cause of deafness (10, 39).

Pendrin belongs to the gene family *SLC26A*, which contains sulfate transporters, and therefore was initially thought to be a transporter for sulfate (10). Subsequent expression studies in *Xenopus laevis* oocytes, Sf9 insect, and HEK-293 cells have shown that pendrin functions as an exchanger that transports anions such as Cl⁻, I⁻, HCO₃⁻, and formate but not sulfate or oxalate (34–36). Functional studies in native tissues have only been performed in the murine renal collecting duct, where pendrin is expressed in β- and non-α-, non-β-intercalated cells (33). Isolated, perfused collecting ducts from NaHCO₃-fed, deoxycorticosterone-treated *Slc26a4*^{-/-} mice reabsorbed HCO₃⁻, whereas ducts from similarly treated *Slc26a4*^{+/+} mice secreted HCO₃⁻, suggesting that pendrin is involved in HCO₃⁻ secretion (33). It is conceivable that pendrin is involved in HCO₃⁻ secretion in the inner ear. Evidence for HCO₃⁻ secretion into endolymph comes from the observations that endolymphatic pH and HCO₃⁻ concentrations are relatively high (15, 16). If pendrin would be involved in HCO₃⁻ secretion, it would be expected that loss of pendrin leads to an acidification of pH. The first aim of the present study was to determine whether pendrin in the inner ear is functional and whether loss of pendrin affects endolymphatic pH.

Pendred syndrome can be associated with deafness at birth or with progressive hearing loss during childhood (6, 41). This implies that hearing develops in at least some cases but is lost during childhood. Compared with humans, the life span of mice is much compressed. Furthermore, mice are born developmentally more immature than humans. Degeneration of the organ of Corti was found in *Slc26a4*^{-/-} mice to begin around the time of the normal onset of hearing. Adult mice were found deaf due to a loss of *Kcnj10* protein expression in the stria vascularis and an ensuing loss of the endocochlear potential, which is the major driving force for sensory transduction (9, 44). The stria vascularis of adult mice was found to degenerate, and this degeneration was found to be associated with an invasion of macrophages (18). Taken together, these findings raised the question of whether *Kcnj10* expression and endocochlear potential are first developed and then lost, which implies the existence of a window of opportunity to intervene

Address for reprint requests and other correspondence: P. Wangemann, Anatomy and Physiology Dept., Kansas State Univ., 205 Coles Hall, Manhattan, KS 66506 (e-mail: wange@vet.ksu.edu).

The costs of publication of this article were defrayed in part by the payment of page charges. The article must therefore be hereby marked “advertisement” in accordance with 18 U.S.C. Section 1734 solely to indicate this fact.

and prevent loss of function. Alternatively, it was conceivable that *Kcnj10* expression and the endocochlear potential failed to develop, which may point to a prenatal defect that would be difficult to correct during postnatal life. Thus the second aim of the present study was to determine whether *Slc26a4*^{-/-} mice develop hearing, express *Kcnj10* in the stria vascularis, and generate an endocochlear potential.

Endolymphatic Ca²⁺ concentration is unusually low for an extracellular fluid, which is critically important for sensory transduction. Reabsorption of Ca²⁺ from vestibular endolymph has recently been shown to involve the epithelial Ca²⁺ channels *Trpv5* and *Trpv6* (*Trpv5* synonyms: *ECaC1* and *CaT2*; *Trpv6* synonyms: *ECaC2*, *CaT1*) (46). The observations that *Trpv5* and *Trpv6* are inhibited by an acidification of extracellular pH (29, 42) and that transepithelial Ca²⁺ absorption in *Trpv5*- and *Trpv6*-expressing rat semicircular canal epithelium was inhibited by extracellular acidification (24) raised the hypothesis that loss of pendrin leads to inhibition of sensory transduction via inhibition of Ca²⁺ absorption and an increase in endolymphatic Ca²⁺ concentration. Thus the third aim of the present study was to determine whether *Trpv5* and *Trpv6* channel proteins are expressed in the cochlea and whether loss of pendrin leads to a change in endolymphatic Ca²⁺ concentration that may present a key event in the etiology of deafness.

METHODS

Animal use. Mongolian gerbils were obtained from a commercial source (Charles River, Wilmington, MA) and housed at Kansas State University (KSU). Adult *Slc26a4*^{-/-} and *Slc26a4*^{+/+} mice were obtained either from the colony of Dr. Susan Wall (Emory University) or from a colony at KSU that was established with breeders kindly provided by Dr. Wall. Prewaning mice and *Slc26a4*^{+/-} mice were solely obtained from the KSU colony. Gerbils were deeply anesthetized with pentobarbital sodium (100 mg/kg ip) and killed by decapitation. Prewaning mice were deeply anesthetized with 4% tribromoethanol (0.013 ml/g body wt ip). Adult mice were deeply anesthetized either with 4% tribromoethanol (0.014 ml/g body wt ip) or with pentobarbital sodium (100 mg/kg body wt ip) and killed by decapitation or transcardial perfusion. All procedures involving animals were approved by the Institutional Animal Care and Use Committee of Kansas State University.

Ratiometric pH measurements. Temporal bones were extracted from gerbils after death, and lateral wall tissues were obtained by microdissection in Cl⁻-free solution. Cl⁻-free solution contained (in mM) 150 Na-gluconate, 1.6 K₂HPO₄, 0.4 KH₂PO₄, 4 Ca-gluconate₂, 1 MgSO₄, and 5 glucose, pH 7.4. Great care was taken to not strip stria vascularis from the underlying spiral ligament. Lateral wall tissues were loaded with BCECF by incubation with 5 μM BCECF-AM for 45 min at 37°C. Tissues were mounted with fine glass needles in a bath chamber installed on the stage of a confocal microscope (PASCAL 5, Carl Zeiss, Jena). For optimal fluorescence imaging, the epithelial side of the tissue faced toward the coverslip. Tissues were initially superfused with 150 Cl⁻ solution that contained (in mM) 150 NaCl, 3.5 KCl, 1 CaCl₂, 1 MgCl₂, and 5 glucose, pH 7.4. Cl⁻ steps from 150 to 15 mM were performed by replacement of 135 mM NaCl with an equimolar amount of Na-gluconate, while increasing the amounts of CaCl₂ and MgCl₂ from 1 to 4 mM to compensate for chelation. Formate (10 mM) and DIDS (1 mM, predissolved in DMSO) were simply added to solutions. Fluorescence originating from surface epithelial cells in the spiral prominence region was recorded without interference of underlying connective tissue or capillary networks. Contributions of connective tissue were excluded since connective tissue cells did not load BCECF under the chosen

conditions. Furthermore, contributions of capillary endothelial cells that loaded BCECF were avoided by choice of an appropriate optical section. Fluorescence was imaged in an alternating manner in response to 458- and 488-nm excitation using the same detector operated at a fixed gain, offset, and amplification. The fluorescence ratio was converted to pH according to a calibration performed in droplets of BCECF acid dissolved in HEPES-buffered solutions of varying pH (Fig. 1).

Electrophysiological pH and Ca²⁺ measurements. The endolymphatic pH and Ca²⁺ concentrations and the endocochlear potential were measured in situ with double-barreled microelectrodes. Procedures were developed by modifying previously described protocols (21). Measurements were made in the basal turn of the cochlea by a round-window approach through the basilar membrane of the first turn. After electrodes were placed in the perilymph, the surgical cavity was covered with liquid Sylgard 184 (Dow Corning, Midland, MI). This maneuver was designed to prevent the measurement of artificially elevated perilymphatic pH values due to the loss of tissue CO₂ into ambient air. Indeed, perilymph values in a preliminary series of experiments that lacked this precaution were significantly higher (7.67 ± 0.04, n = 8 vs. 7.33 ± 0.04, n = 11).

Calibration consisted of taking a reference value and obtaining the slope of the electrode in an agar cup in situ. This method was devised to minimize the contribution of electrode drift and differences between reference electrodes. After cochlear measurements of endolymph and perilymph, the surgical cavity was flooded with pH 7 or 1 mM Ca²⁺ calibration solutions and the electrode was lifted through the Sylgard layer to rapidly obtain a reference measurement. Subsequently, the slope of the electrode was obtained by placing an agar cup on the exposed neck muscles and connecting it to three inflow lines for calibration solutions and one suction line. The electrode was moved into the cup, and the tip was perfused with calibration solutions (1 min/solution). Agar cups holding ~100 μl were prepared with weakly buffered Ringer solution. Slopes of Ca²⁺- and pH-sensitive electrodes were 25.0 ± 0.6 mV/decade concentration (n = 19) and 57.1 ± 0.3 mV/pH unit (n = 24), respectively.

Double-barreled glass microelectrodes were manufactured from filament-containing glass tubing (1B100F-4, World Precision Instruments, Sarasota, FL) using a micropipette puller (Narishige PD-5, Tokyo, Japan). Before silanization, microelectrodes were baked at 180°C for 2 h to ensure dryness. The longer ion-selective barrel was mounted in the lid of a beaker. The beaker was heated to 210°C and silanized by a 90-s exposure to 0.08 ml dimethyldichlorosilane (Fluka 40136) at room temperature. The shorter reference barrel was protected from silanization by sealing the open end with Parafilm (Alcan Packaging, Chicago, IL). After silanization, microelectrodes were baked at 180°C for 3 h and tips were broken to a final outer diameter of ~3 μm. For pH electrodes, the reference barrel was filled with 1 M KCl and the

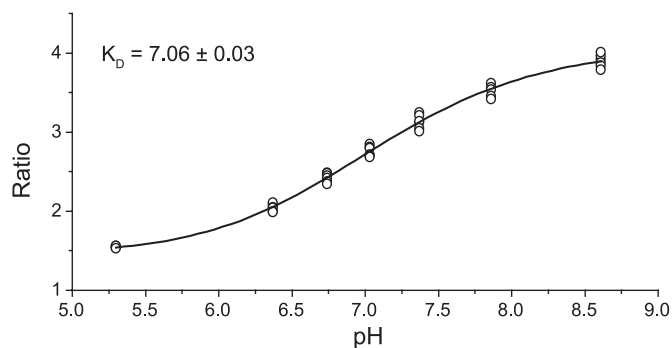


Fig. 1. Calibration of ratiometric pH measurements. The ratio of fluorescent emissions of BCECF is plotted against various pH values. Fluorescence emissions were detected in response to excitation using the 458- and 488-nm lines of an argon laser. The K_d of 7.06 ± 0.03 is close to the theoretical value of 7.0.

ion-selective barrel was filled at the tip with liquid ion exchanger (Fluka 95297, Hydrogen ionophore II-Cocktail A) and back-filled with buffer solution (500 mM KCl, 20 mM HEPES, pH 7.34). For Ca²⁺ electrodes, the reference barrel was filled with 150 mM KCl and the ion-selective barrel was filled at the tip with liquid ion exchanger (Fluka 21048, Calcium ionophore I-Cocktail A) and back-filled with 500 mM CaCl₂. Each barrel was connected to an input of a grounded dual electrometer (FD223, World Precision Instruments) via Ag-AgCl wire electrodes. The animal was grounded via a Ag-AgCl wire electrode inserted into the neck musculature. Current pulses (1 nA) were injected via the reference barrel to monitor electrode resistance.

pH-sensitive electrodes were calibrated using solutions of three different pH values (in mM): pH 6: 130 NaCl, 20 MES; pH 7: 130 NaCl, 20 HEPES; and pH 8: 130 NaCl, 20 tricine. Ca²⁺-sensitive electrodes were calibrated using solutions of three different Ca²⁺ concentrations (mM): 0.01 mM Ca²⁺: 150 KCl, 0.121 CaCl₂, 10 HEPES, 1 nitrilotriacetic acid (Sigma N-0128, Ca²⁺ buffer), pH 7.4; 0.1 mM Ca²⁺: 150 KCl, 0.1 CaCl₂, 10 HEPES, pH 7.4; and 1 mM Ca²⁺: 150 KCl, 1 CaCl₂, 10 HEPES, pH 7.4.

Data were recorded analog (Flat Bed Chart recorder, Kipp & Zonen) for convenient annotation and digital for presentation and data analysis (DIGIDATA 1322A and AxoScope 9, Axon Instruments). Data were analyzed using custom software written by P. Wangemann in LabTalk (Origin 6.0, The Origin, Northampton, MA).

Measurements of the endocochlear potential were reduced by 1.3 and 4.2 mV to correct for the liquid junction potentials that occur by advancing the electrode filled with 1 M KCl or 150 mM KCl from perilymph (150 NaCl) to endolymph (150 mM KCl). Similar corrections were also made to the measurements of the endolymphatic pH and the perilymphatic Ca²⁺ concentration since pH and Ca²⁺ measurements were calibrated with NaCl- and KCl-containing solutions, respectively.

Blood electrolyte measurements. Plasma profiles were obtained using a blood analyzer (Stat Profile M, Nova Biomedical, Waltham, MA). No significant differences were found between *Slc26a4*^{+/-} and *Slc26a4*^{+/+} mice (Table 1).

Auditory brain stem recordings. Mice were deeply anesthetized with 4% tribromoethanol (0.013–0.014 ml/g body wt ip) and placed on a thermal pad to maintain normal body temperature. The mastoid, vertex, and ventral neck region of the animal were connected via subdermal platinum needle electrodes (F-E2, Astro-Med, West Warwick, RI) and short (31 cm) leads to the main channel, reference channel, and ground of the preamplifier, respectively. Auditory brain stem recordings were performed in a custom constructed, electrically shielded, and sound-attenuated chamber (inner dimensions 23 × 23 × 23 cm) using a digital data-acquisition system (BioSig32 software, RA4LI Preamplifier, RP2.1 Enhanced Real Time Processor, PA5 Programmable Attenuator, ED1 Electrostatic Speaker Driver, Tucker-Davis Technologies, Alachua, FL). Tone burst and click stimuli were presented (21/s) via a free-field electrostatic speaker (SigGen software, ES1 speaker, Tucker-Davis). Acoustic stimuli were calibrated using a 1/4-in. condenser microphone (SigCal IRP4.2 software, Tucker-Davis; PS9200 microphone, Acoustical Interface, Belmont, CA) that replaced the mouse's head. Clicks (1-ms duration) and tone bursts (2-ms duration, 0.5-ms gate time; 8, 16, and 32 kHz) were presented with alternating phase (0 and 180°). Responses, recorded over 10 ms, were filtered (300-Hz high pass, 3,000-Hz low pass, and 60-Hz

notch), and 1,000 recordings were averaged. Click and tone burst stimuli were presented at intensities varying between 90 and 10 dB SPL in 10-dB intervals. Auditory thresholds were obtained by a visual comparison of waveforms.

Immunocytochemistry. Mice were deeply anesthetized and killed by transcardial perfusion with Cl⁻-free or NaCl solution (6 ml, 1 min) followed by Cl⁻-free or NaCl solution with 4% paraformaldehyde (24 ml, 4 min). Cl⁻-free solution contained (mM) 150 Na-gluconate, 1.6 K₂HPO₄, 0.4 KH₂PO₄, 4 Ca-gluconate, 1 MgSO₄, and 5 glucose, pH 7.4. NaCl solution contained (mM) 150 NaCl, 1.6 K₂HPO₄, 0.4 KH₂PO₄, 0.7 CaCl₂, 1 MgCl₂, and 5 glucose, pH 7.4. Cryosection and whole mounts of stria vascularis were prepared.

For cryosections, temporal bones were decalcified in 10% EDTA, processed through a sucrose gradient, and infiltrated with polyethylene glycol. Midmodiolar cryosections (12 μm, CM3050S, Leica, Nussloch, Germany) were blocked in PBS-TX (137 mM NaCl, 10.1 mM Na₂HPO₄, 1.8 mM KH₂PO₄, 2.7 mM KCl, pH 7.4, with 0.2% Triton X-100) and 5% bovine serum albumin. Slides were incubated overnight at 4°C with primary antibody in PBS-TX with 1–3% BSA. Primary antibodies included rabbit anti-*pendrin* (1:500, h766–780, a kind gift from Dr. Ines Royaux, National Institutes of Health), goat anti-*Kcnj1* (1:200, C20, Santa Cruz Biotechnology, Santa Cruz, CA), rabbit anti-*Kcnj10* antibody (1:300, Alomone, Jerusalem, Israel), rabbit anti-rat *Trpv5* (1:100, CAT21-A, Alpha Diagnostics, San Antonio, TX), and rabbit anti-rat *Trpv6* (1:100, Alpha Diagnostics). Slides were washed in PBS-TX and incubated for 1 h at room temperature with secondary antibodies at a 1:1,000 dilution in PBS-TX with 1–3% BSA. Secondary antibodies included donkey anti-rabbit Alexa 488 and chicken anti-goat Alexa 594 (Molecular Probes, Eugene, OR). After incubation, slides were washed with PBS-TX and mounted with FluorSave (Calbiochem, La Jolla, CA).

For whole mounts, the stria vascularis was isolated by microdissection and postfixed for 2 h at 4°C in Cl⁻-free solution containing 4% paraformaldehyde. Fixed stria vascularis was washed 2× in Cl⁻-free solution and 1× in PBS-TX and blocked with 5% BSA in PBS-TX for 45 min at room temperature and again washed 3× in PBS-TX. The tissue was then incubated overnight at 4°C with anti-*Kcnj10* antibody (1:300; see above) in PBS-TX with 1–3% BSA, washed with PBS-TX, and incubated for 1 h at room temperature with donkey anti-rabbit Alexa 488 secondary antibody (1:1,000, Molecular Probes) in PBS-TX with 1–3% BSA. After antibody incubation, the stria vascularis was washed 3× in PBS-TX and mounted with FluorSave between two coverslips.

Cryosections and whole mounts were viewed by confocal microscopy (LSM 510 Meta, Carl Zeiss, Göttingen, Germany). Laser-scanning brightfield images were collected to aid orientation and document structural preservation.

Statistics. Data are given as average ± SE. Differences were determined by paired and unpaired *t*-test, as appropriate. Significance was assumed at *P* < 0.05.

RESULTS

***Pendrin* protein expression in the cochlea is functional.** *Pendrin* has been shown to be expressed in the apical membrane of endolymph-facing, spiral prominence epithelial cells

Table 1. Analysis of blood plasma from *Slc26a4*^{+/+} and *Slc26a4*^{-/-} mice

	pH	Na, mmol/l	K, mmol/l	Cl, mmol/l	Ca, mg/dl	Glucose, mg/dl	Lactate, mmol/l	Osmolality, mosmol/kgH ₂ O
<i>Slc26a4</i> ^{+/+} (n = 7)	7.18 ± 0.02	156.7 ± 1.6	4.9 ± 0.3	117.1 ± 1.6	2.6 ± 0.5	145 ± 24	2.6 ± 0.4	317 ± 3
<i>Slc26a4</i> ^{-/-} (n = 6)	7.21 ± 0.02	160.2 ± 1.9	5.1 ± 0.3	116.3 ± 2.6	2.6 ± 0.4	118 ± 15	2.3 ± 0.4	319 ± 4

(44). When expressed in heterologous expression systems, pendrin has been shown to mediate formate-enhanced and DIDS-sensitive cytosolic alkalinizations in response to reductions in the extracellular Cl^- concentration (34, 36). Similar protocols were used here to evaluate whether pendrin expressed in the cochlea is functional. Spiral prominence regions of the gerbil cochlea were isolated, and surface epithelial cells were loaded with BCECF (Fig. 2). Reductions in extracellular Cl^- concentration from 150 to 15 mM in the absence of formate resulted in a cytosolic alkalinization by 0.13 ± 0.02 pH units (29 cells in 8 preparations). Addition of 1 or 10 mM formate resulted in an acidification by 0.03 ± 0.01 (9 cells in 2 preparations) and 0.12 ± 0.02 pH units (14 cells in 4 preparations), respectively. Addition of 1 mM DIDS had no significant effect (-0.03 ± 0.02 pH units, 13 cells in 2

preparations). Paired experiments revealed that Cl^- -induced alkalinizations were enhanced by 10 mM formate and inhibited by 1 mM DIDS. These observations are consistent with the presence of functional pendrin protein in the cochlea.

Mice lacking pendrin do not develop hearing. Inner and outer hair cells in the organ of Corti have been shown to develop normally in *Slc26a4*^{-/-} mice but to begin to degenerate between postnatal day 7 (P7) and P15, which encompasses the onset of hearing at P12 (9). These observations raised the hypothesis that *Slc26a4*^{-/-} mice may develop hearing for at least a brief period. Hearing was evaluated by auditory brain stem response thresholds in *Slc26a4*^{+/-} and *Slc26a4*^{-/-} mice. *Slc26a4*^{+/-} mice began hearing at P12, with the threshold improving daily (Fig. 3). In contrast, *Slc26a4*^{-/-} lacked hearing at all ages tested. The equivalency of develop-

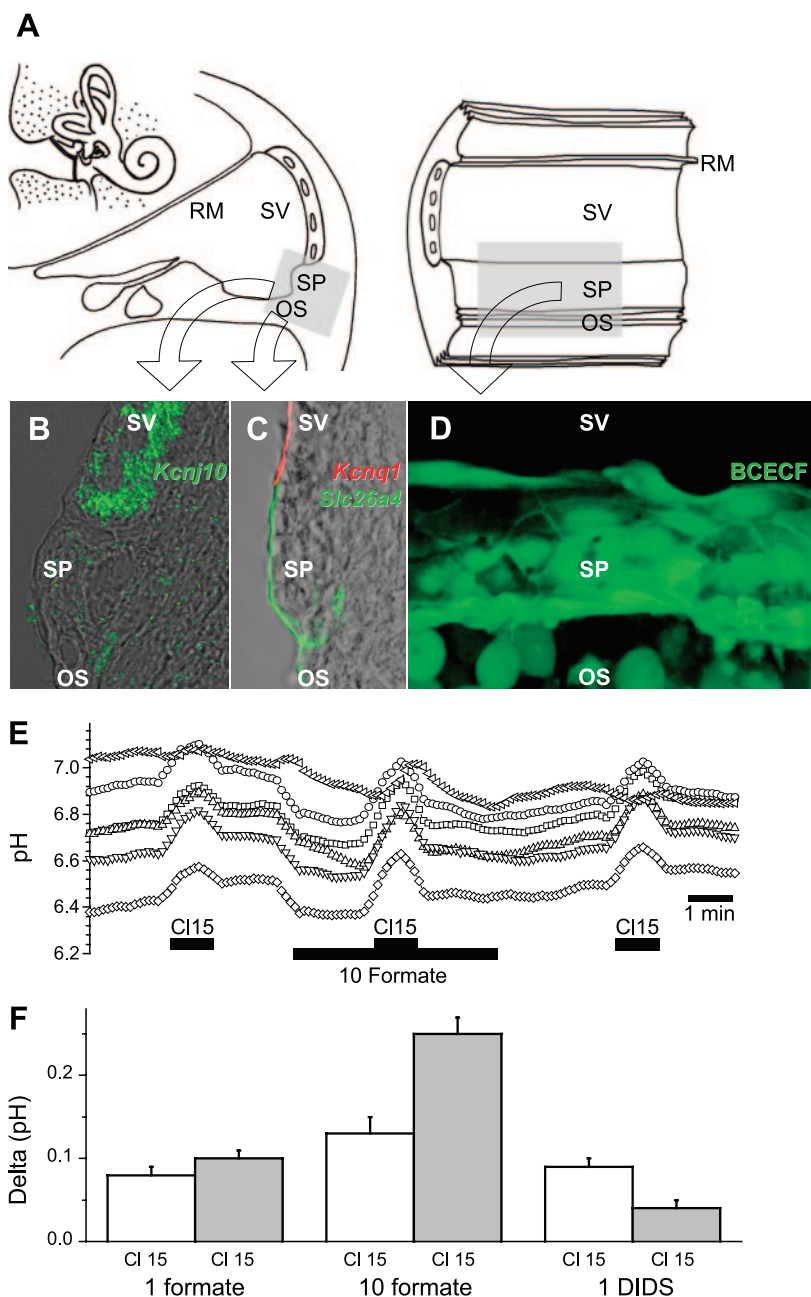


Fig. 2. Ratiometric pH measurements in pendrin-expressing spiral prominence epithelial cells from a gerbil. *A*: location and microdissection of spiral prominence (SP), outer sulcus (OS), and stria vascularis (SV). RM, Reissner's membrane. *B* and *C*: expression of *Kcnj10*, *Kcnq1*, and Pendrin in the SP region of the lateral wall. Confocal immunohistochemistry of cryosections is shown. *Kcnj10* was expressed in intermediate cells of the stria vascularis, and *Kcnq1* in the apical membrane marginal cells of the SV and pendrin in the apical membrane of SP epithelial cells. Pendrin-expressing cells were clearly distinct from marginal and intermediate cells of the SV. *D*: SP epithelial cells were loaded with BCECF. OS cells suffered from damage received during microdissection, and marginal cells of the SV did not load BCECF under the conditions chosen. *E*: cellular pH measurements. Cl^- concentration steps from 150 to 15 mM (CI15) caused an alkalinization that was enhanced in the presence of 10 mM formate. *F*: data summary. Cl^- step-induced cellular alkalinization was enhanced by 10 mM formate and inhibited by 1 mM DIDS.

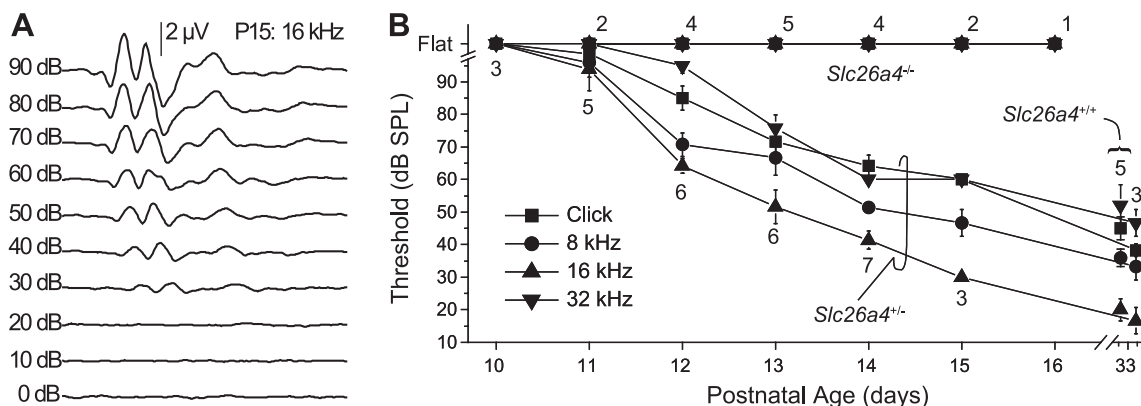


Fig. 3. Evaluation of hearing in *Slc26a4*^{+/+} and *Slc26a4*^{-/-} mice. Hearing thresholds were determined by auditory brain stem recordings using click and tone-burst stimuli at 8, 16, and 32 kHz. *A*: example of auditory brain stem recordings made in a postnatal day 15 (P15) *Slc26a4*^{+/+} mouse using 16-kHz tone-burst stimuli at different amplitudes. *B*: data summary. The onset of hearing occurred in *Slc26a4*^{+/+} mice at P12. Hearing in *Slc26a4*^{+/+} mice improved daily, reaching nearly adult levels by P15. *Slc26a4*^{-/-} mice did not develop hearing.

ment was evaluated by observing the time of eye opening. No difference in eye opening was found among *Slc26a4*^{+/+}, *Slc26a4*^{+/-}, and *Slc26a4*^{-/-} mice (11.3 ± 0.2 , $n = 7$; 11.5 ± 0.1 , $n = 41$; and 11.5 ± 0.1 postnatal days, $n = 26$, respectively).

Lack of pendrin leads to loss of Kcnj10 and endocochlear potential. We have shown previously that adult *Slc26a4*^{-/-} mice lack protein expression of the K⁺ channel *Kcnj10* in the stria vascularis and consequently do not generate an endocochlear potential (44). The finding raised the question of whether *Slc26a4*^{-/-} mice never express *Kcnj10* in the stria vascularis or whether these mice first express *Kcnj10* and then lose expression. This question was addressed by measuring the endocochlear potential and *Kcnj10* expression in stria vascularis before and after the onset of hearing. *Slc26a4*^{-/-} mice developed a small endocochlear potential at P10 that was progressively lost during further development (Fig. 4). Consistent with this observation, *Kcnj10* was expressed at P10 and was progressively lost during further development (Fig. 5).

Lack of pendrin causes acidification of endolymphatic pH. The observations that pendrin is expressed in the apical membrane of spiral prominence epithelial cells and that pendrin is an anion exchanger that accepts pH equivalents raised the hypothesis that pendrin controls endolymphatic pH. pH was measured with double-barreled ion-selective electrodes in endolymph and perilymph of *Slc26a4*^{+/+} and *Slc26a4*^{-/-} mice. Measurements were made before and after the onset of hearing. At all ages, endolymph of *Slc26a4*^{+/+} mice was more alkaline than perilymph. In contrast, endolymph of *Slc26a4*^{-/-} mice was more acidic than perilymph (Fig. 6). No difference was found in the pH of perilymph or blood between *Slc26a4*^{+/+} and *Slc26a4*^{-/-} mice (Fig. 6, Table 1).

Cochlear epithelial cells express Ca²⁺ channels Trpv5 and Trpv6. Epithelial Ca²⁺ channels *Trpv5* and *Trpv6* have recently been found to contribute to Ca²⁺ reabsorption from vestibular endolymph (24, 46). This finding raised the question of whether these channels are also expressed in cochlear epithelial cells and contribute to Ca²⁺ absorption in the cochlea. Expression of *Trpv5* was mainly found in marginal cells of stria vascularis, and expression of *Trpv6* was found mainly in inner and outer sulcus epithelial cells (Fig. 7). Staining for

Trpv5 and *Trpv6* was similar in *Slc26a4*^{+/+} and *Slc26a4*^{-/-} mice.

Lack of pendrin causes elevation of endolymphatic Ca²⁺ concentration. Ca²⁺ concentration was measured with double-barreled ion-selective electrodes in endolymph and perilymph of *Slc26a4*^{+/+} and *Slc26a4*^{-/-} mice before and after the onset of hearing. At P10, Ca²⁺ concentration in endolymph of *Slc26a4*^{+/+} mice was lower than Ca²⁺ concentration in perilymph. During further development, endolymphatic Ca²⁺ concentration progressively decreased to adult levels (Fig. 6). In contrast, endolymphatic Ca²⁺ concentration in *Slc26a4*^{-/-} mice at P10 was similar to Ca²⁺ concentration in perilymph. During further development, endolymphatic Ca²⁺ concentration progressively increased. No difference was found in Ca²⁺ concentration of perilymph or blood between *Slc26a4*^{+/+} or *Slc26a4*^{-/-} mice (Fig. 6, Table 1).

DISCUSSION

The most salient findings of the present study are as follows. 1) Pendrin in spiral prominence epithelial cells of the cochlea is a functional anion exchanger. 2) At P10, before the onset of hearing, *Slc26a4*^{-/-} mice express *Kcnj10* in the stria vascularis and generate a small endocochlear potential. During further development, *Kcnj10* expression and endocochlear po-

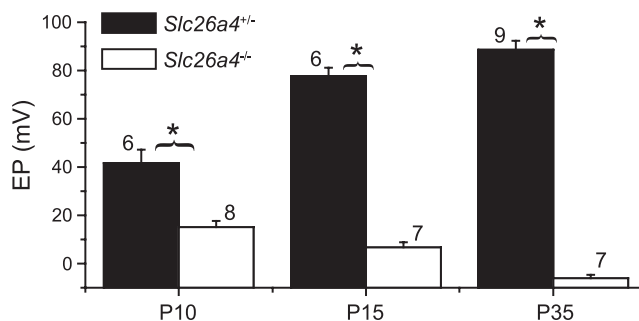


Fig. 4. Measurements of endocochlear potential (EP) in *Slc26a4*^{+/+} and *Slc26a4*^{-/-} mice before and after the onset of hearing. At P10, *Slc26a4*^{+/+} and *Slc26a4*^{-/-} mice generated an endocochlear potential. This potential grew with further development in *Slc26a4*^{+/+} mice but was lost in *Slc26a4*^{-/-} mice. * $P < 0.05$.

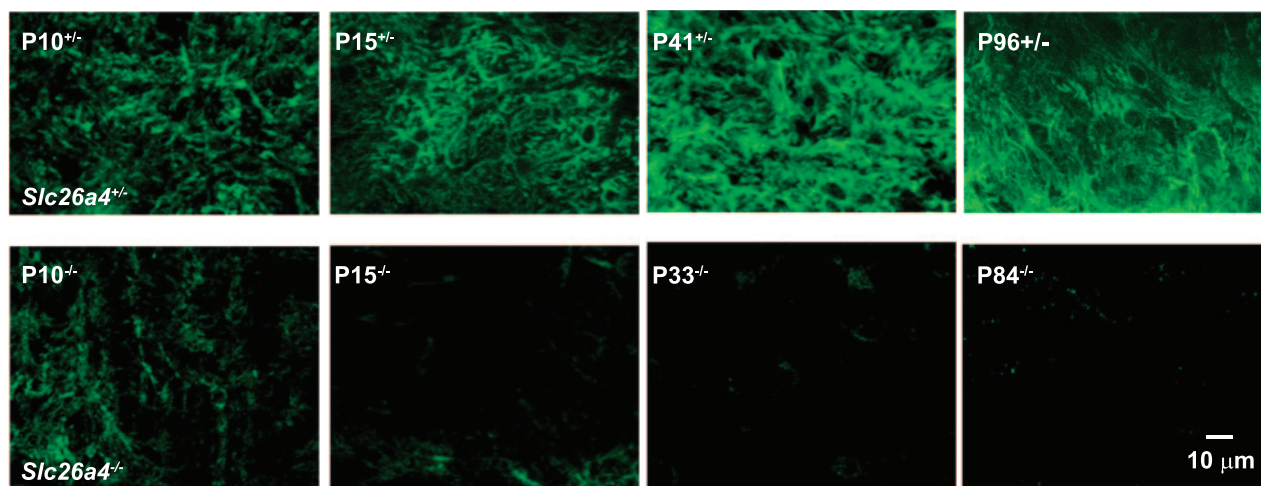


Fig. 5. Development of expression of K^+ channel *Kcnj10* in SV of *Slc26a4*^{+/+} and *Slc26a4*^{-/-} mice. Confocal immunohistochemistry of whole mounts of SV is shown. *Top*: images from *Slc26a4*^{+/+} mice of various ages. *Bottom*: images from *Slc26a4*^{-/-} mice. The scale bar shown in the *bottom right* image represents 10 μm and pertains to all images in this figure.

tential are lost and *Slc26a4*^{-/-} mice fail to develop hearing. 3) Lack of pendrin leads to an acidification and an increase in the Ca^{2+} concentration of endolymph. 4) Epithelial cells enclosing endolymph express the acid-sensitive Ca^{2+} channels *Trpv5* and *Trpv6* in the apical membrane.

Pendrin mediates HCO_3^- secretion into endolymph. The observation that pendrin is a functional anion exchanger and that loss of pendrin leads to an acidification of endolymph suggests that the main anions transported are alkaline equivalents such as HCO_3^- . HCO_3^- is a likely substrate for pendrin

since the stria vascularis generates CO_2 and the spiral prominence is heavily expressing carbonic anhydrase, which converts CO_2 to HCO_3^- (14, 26). The stria vascularis is a source of CO_2 because it has a higher metabolic rate than neighboring tissues and because it has a respiratory quotient of 1.2, which means that it generates 1.2 CO_2 for every O_2 molecule consumed (22). In addition, spiral ligament and spiral prominence fibrocytes express *Slc4a7*, which is a $\text{Na}^+/\text{HCO}_3^-$ cotransporter likely involved in the uptake of HCO_3^- into cells (3). Consistent with pendrin-mediated HCO_3^- secretion is the observation

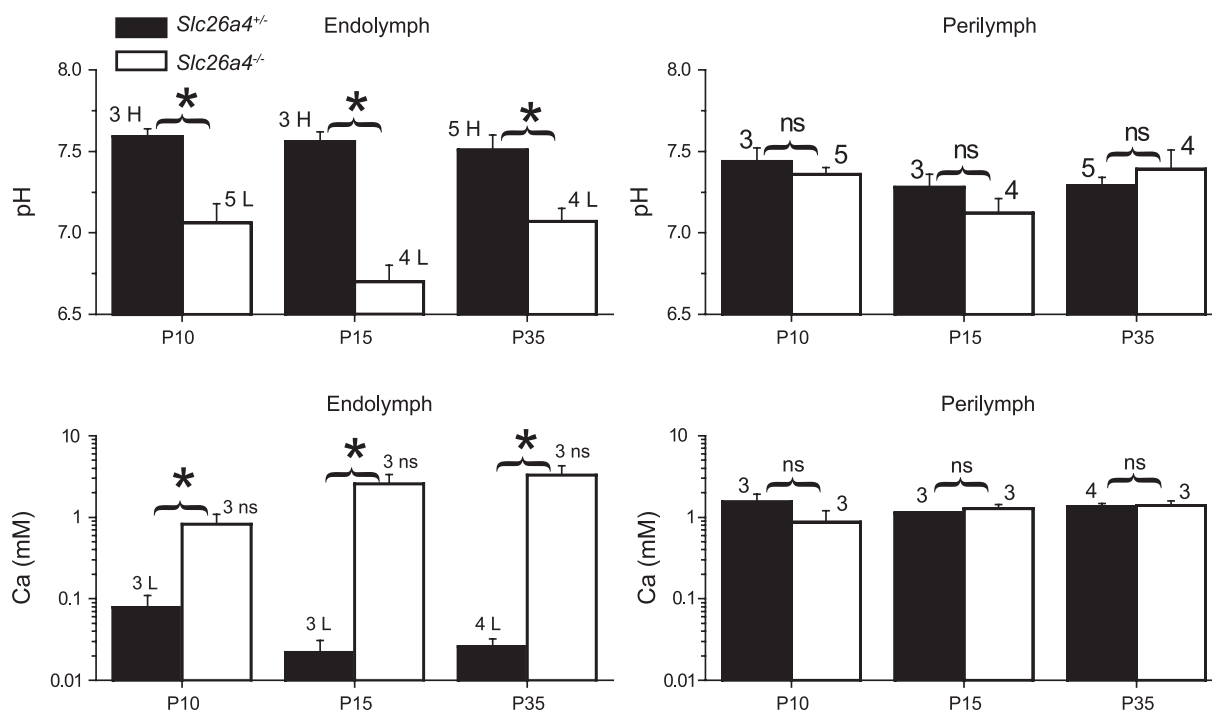


Fig. 6. Measurements of the endolymphatic and perilymphatic pH and Ca^{2+} concentration in *Slc26a4*^{+/+} and *Slc26a4*^{-/-} mice before and after the onset of hearing. At all ages, the endolymphatic pH compared with the perilymphatic pH was more alkaline in *Slc26a4*^{+/+} mice and more acidic in *Slc26a4*^{-/-} mice. With development, the endolymphatic Ca^{2+} concentration decreased in *Slc26a4*^{+/+} and increased in *Slc26a4*^{-/-} mice. Significant differences between endolymph and perilymph are marked (H, higher in endolymph; L, lower in endolymph). *Significant differences between *Slc26a4*^{+/+} and *Slc26a4*^{-/-} (* $P < 0.05$). Insignificant differences are marked (ns). Numbers next to error bars represent the number of animals.

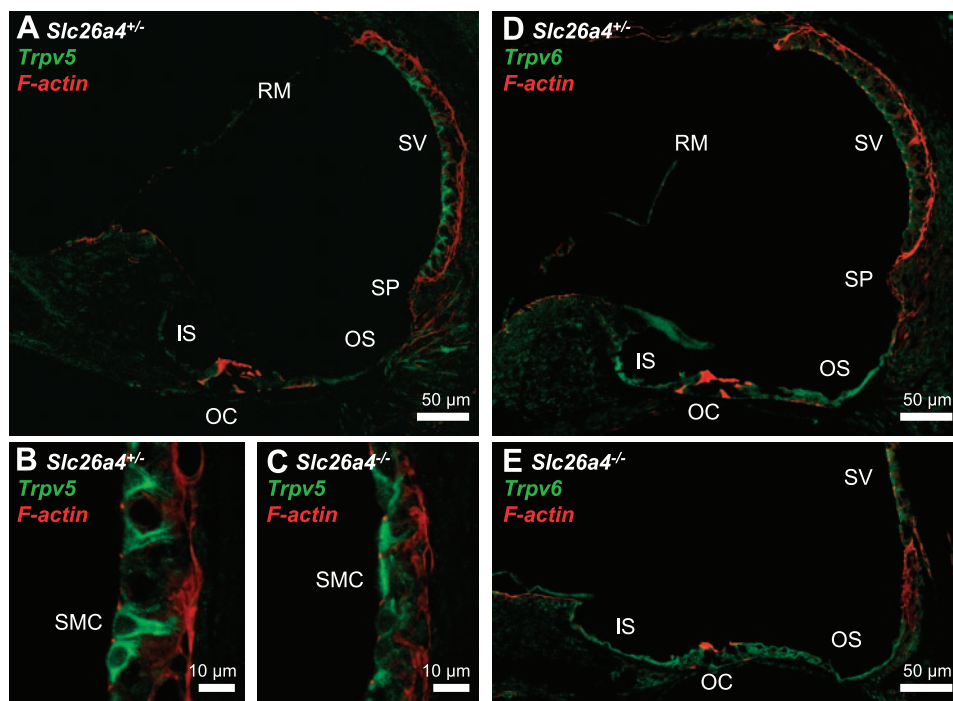


Fig. 7. Expression of the Ca²⁺ channels *Trpv5* (A–C) and *Trpv6* (D and E) in the cochlea of *Slc26a4*^{+/-} and *Slc26a4*^{-/-} mice at P16. Confocal immunohistochemistry of cryosections is shown. *Trpv5* was mainly expressed in SV and less in inner sulcus (IS) and OS epithelial cells. *Trpv6* was expressed mainly expressed in IS and OS epithelial cells and less in SV. Expression found in *Slc26a4*^{+/-} mice was also found in *Slc26a4*^{-/-} mice. Phalloidin-based staining of F-actin was used to provide orientation within the sections.

that the HCO₃⁻ concentration in endolymph is higher than in perilymph and that inhibition of carbonic anhydrase leads to an acidification of endolymph and a reduction in HCO₃⁻ (16, 38). Furthermore, acoustic stimulation, which increases metabolism and CO₂ production, has been shown to cause an alkalization of endolymph (15).

Coincidentally, pendrin-mediated HCO₃⁻ secretion has recently been demonstrated in the cortical collecting duct of the kidney (33). A systemic effect as origin of the acidified endolymphatic pH, however, is unlikely since no difference in plasma or perilymphatic pH was observed.

In the absence of pendrin, endolymph was more acidic than perilymph. Acid secretion into endolymph, which was uncovered in the absence of pendrin, may occur in several endolymph-facing epithelial cells, including cochlear interdental cells, known to express the subunits E and B1 of the vH⁺-ATPases in the apical membrane and the Cl⁻/HCO₃⁻ exchanger *Slc4a2* (AE2) in the basolateral membrane (19, 37). Additional acid secretion sites may include stria marginal cells, which express the E subunit of the vH⁺-ATPases in their apical membrane (37).

The possibility that the endocochlear potential would provide a driving force for pH equivalents and that loss of the endocochlear potential in *Slc26a4*^{-/-} mice would be the sole cause for endolymphatic acidification is unlikely since a similar acidification of endolymph was found in the vestibular labyrinth, although there is no difference in the transepithelial voltage between *Slc26a4*^{+/-} and *Slc26a4*^{-/-} mice (24). HCO₃⁻ secretion into vestibular endolymph is likely mediated by pendrin expressed in vestibular transitional cells (44).

Early loss of Kcnj10 prevents the development of hearing. The endocochlear potential, which is generated by the K⁺ channel *Kcnj10*, is crucial for hearing since it drives sensory transduction (23, 43). Adult *Slc26a4*^{-/-} mice lack *Kcnj10* protein expression and fail to generate an endocochlear poten-

tial, which is consistent with the fact that adult *Slc26a4*^{-/-} mice are deaf (9, 44).

In general, mice are born blind and deaf. Eyes and ear canals open at P11, and hearing begins at P12. Expression of the K⁺ channel *Kcnj10* in the stria vascularis begins in mice around P8, and the onset of expression is paralleled by the onset of an endocochlear potential (13). At P10, *Slc26a4*^{-/-} mice express a small endocochlear potential. This finding demonstrates that the stria vascularis of *Slc26a4*^{-/-} mice can express *Kcnj10* protein and can generate an endocochlear potential.

A window of opportunity may exist to prevent loss of *Kcnj10* expression and to enable *Slc26a4*^{-/-} mice to develop a normal endocochlear potential and normal hearing. This narrow window of opportunity appears to close with the degeneration of the organ of Corti that begins between P7 and P15 (9). Pendrin and *Kcnj10* are expressed in different cells. The link between loss of pendrin function and loss of *Kcnj10* expression remains unclear.

Endolymphatic acidification inhibits Ca²⁺ absorption. Under physiological conditions, endolymphatic Ca²⁺ concentration is 20–30 μM, which is very low for an extracellular compartment (4). Higher or lower concentrations have been shown to suppress transduction currents and microphonic potentials (25, 40). The endolymphatic Ca²⁺ concentration is likely controlled by secretory and absorptive processes. Ca²⁺ secretion may involve basolaterally expressed Ca²⁺ influx mechanisms in conjunction with apically expressed Ca²⁺-ATPases such as PMCA2 (45). Support for active Ca²⁺ secretion into endolymph comes from the finding that pharmacological inhibition of Ca²⁺-ATPases leads to a fall in endolymphatic Ca²⁺ concentration (17) and that deaf-waddler mice, which bear a loss-of-function mutation in the apically expressed Ca²⁺-ATPase PMCA2, have a very low endolymphatic Ca²⁺ concentration (45).

Reabsorption of Ca²⁺ may entail apically expressed Ca²⁺ channels *Trpv5* and *Trpv6* in conjunction with basolaterally expressed Ca²⁺-ATPases and Na⁺/Ca²⁺ exchangers (27, 45, 46). The finding that *Trpv5* is expressed in the apical membrane of stria marginal cells in conjunction with the finding of the Ca²⁺-ATPase PMCA1 in their basolateral membrane (45) suggests that the stria vascularis is involved in Ca²⁺ reabsorption. Expression of *Trpv5* and *Trpv6* is of great interest in view that these channels are inhibited by extracellular acidification (29, 42). Endolymphatic acidification may inhibit Ca²⁺ absorption and lead to the observed elevation in endolymphatic Ca²⁺ concentration. The majority of Ca²⁺ that enters the hair cell bundle through the transduction channel under physiological conditions is extruded by Ca²⁺-ATPases that are expressed in the hair cell bundle (47). Although Ca²⁺ is necessary to maintain the sensitivity of the bundle through adaptation and motility (1, 5, 8), an entry of excess Ca²⁺ into the sensory cells leads to Ca²⁺ overloading and cell death. The capacity of cochlear hair cells to extrude Ca²⁺ may be limited, especially in outer hair cells that appear to not express plasma membrane Ca²⁺-ATPases in their basolateral membrane (7). Ca²⁺ overload may be the cause of cellular degeneration that was observed to begin with outer hair cells between *P7* and *P15* (9).

In conclusion, our data demonstrate that pendrin is a functional formate-permeable and DIDS-sensitive anion exchanger that likely mediates HCO₃⁻ secretion into endolymph. Hence endolymph is alkaline, and loss of the pendrin leads to acidification. Endolymphatic acidification may be responsible for inhibition of Ca²⁺ reabsorption via the acid-sensitive Ca²⁺ channels *Trpv5* and *Trpv6*. Failure to lower endolymphatic Ca²⁺ may inhibit sensory transduction necessary for hearing and promote the degeneration of the sensory cells. Degeneration of the sensory cells closes a window of opportunity to restore the normal development of hearing in *Slc26a4*^{-/-} mice and possibly human patients suffering from Pendred syndrome.

ACKNOWLEDGMENTS

The authors thank Dr. Alexander Gow (Wayne State University), Dr. Alec Salt (Washington University), and Andrew Hoyard (Tucker Davis Technologies, Alachua, FL) for valuable help in setting up auditory brain stem recordings at Kansas State University. This work would not have been possible without the dedication of Susan Rose, James Dille, Britt Neely, and Dr. Bart Carter from the Animal Resource Department at the Kansas State University College of Veterinary Medicine.

GRANTS

The support by National Institutes of Health (NIH) research Grants R01-DC-01098 to P. Wangemann and R01-DC-00212 to D. C. Marcus and of the confocal and the molecular biology core facilities through KSU-COBRE NIH Grant P20-RR-017686 is gratefully acknowledged.

REFERENCES

- Benser ME, Marquis RE, Hudspeth AJ. Rapid, active hair bundle movements in hair cells from the bullfrog's sacculus. *J Neurosci* 16: 5629–5643, 1996.
- Bidart JM, Lacroix L, Evain-Brion D, Caillou B, Lazar V, Frydman R, Bellet D, Filetti S, Schlumberger M. Expression of Na⁺/I⁻ symporter and Pendred syndrome genes in trophoblast cells. *J Clin Endocrinol Metab* 85: 4367–4372, 2000.
- Bok D, Galbraith G, Lopez I, Woodruff M, Nusinowitz S, Beltrandel-Rio H, Huang W, Zhao S, Geske R, Montgomery C, Van S, I, Friddle C, Platt K, Sparks MJ, Pushkin A, Abuladze N, Ishiyama A, Dukkipati R, Liu W, Kurtz I. Blindness and auditory impairment caused by loss of the sodium bicarbonate cotransporter NBC3. *Nat Genet* 34: 313–319, 2003.
- Bosher SK, Warren RL. Very low calcium content of cochlear endolymph, an extracellular fluid. *Nature* 273: 377–378, 1978.
- Crawford AC, Evans MG, Fettiplace R. The actions of calcium on the mechano-electrical transducer current of turtle hair cells. *J Physiol* 434: 369–398, 1991.
- Cremers CW, Admiraal RJ, Huygen PL, Bolder C, Everett LA, Joosten FB, Green ED, Van Camp G, Otten BJ. Progressive hearing loss, hypoplasia of the cochlea and widened vestibular aqueducts are very common features in Pendred's syndrome. *Int J Pediatr Otorhinolaryngol* 45: 113–123, 1998.
- Crouch JJ, Schulte BA. Expression of plasma membrane Ca-ATPase in the adult and developing gerbil cochlea. *Hear Res* 92: 112–119, 1995.
- Eatock RA, Corey DP, Hudspeth AJ. Adaptation of mechano-electrical transduction in hair cells of the bullfrog's sacculus. *J Neurosci* 7: 2821–2836, 1987.
- Everett LA, Belyantseva IA, Noben-Trauth K, Cantos R, Chen A, Thakkar SI, Hoogstraten-Miller SL, Kachar B, Wu DK, Green ED. Targeted disruption of mouse Pds provides insight about the inner-ear defects encountered in Pendred syndrome. *Hum Mol Genet* 10: 153–161, 2001.
- Everett LA, Glaser B, Beck JC, Idol JR, Buchs A, Heyman M, Adawi F, Hazani E, Nassir E, Baxevanis AD, Sheffield VC, Green ED. Pendred syndrome is caused by mutations in a putative sulphate transporter gene (PDS). *Nat Genet* 17: 411–422, 1997.
- Everett LA, Morsli H, Wu DK, Green ED. Expression pattern of the mouse ortholog of the Pendred's syndrome gene (Pds) suggests a key role for pendrin in the inner ear. *Proc Natl Acad Sci USA* 96: 9727–9732, 1999.
- Fugazzola L, Mannavola D, Cerutti N, Maghnie M, Pagella F, Bianchi P, Weber G, Persani L, Beck-Peccoz P. Molecular analysis of the Pendred's syndrome gene and magnetic resonance imaging studies of the inner ear are essential for the diagnosis of true Pendred's syndrome. *J Clin Endocrinol Metab* 85: 2469–2475, 2000.
- Hibino H, Higashi-Shingai K, Fujita A, Iwai K, Ishii M, Kurachi Y. Expression of an inwardly rectifying K⁺ channel, Kir5.1, in specific types of fibrocytes in the cochlear lateral wall suggests its functional importance in the establishment of endocochlear potential. *Eur J Neurosci* 19: 76–84, 2004.
- Hsu CJ, Nomura Y. Carbonic anhydrase activity in the inner ear. *Acta Otolaryngol Suppl (Stockh)* 418: 1–42, 1985.
- Ikeda K, Kusakari J, Takasaka T. Ionic changes in cochlear endolymph of the guinea pig induced by acoustic injury. *Hear Res* 32: 103–110, 1988.
- Ikeda K, Kusakari J, Takasaka T, Saito Y. Early effects of acetazolamide on anionic activities of the guinea pig endolymph: evidence for active function of carbonic anhydrase in the cochlea. *Hear Res* 31: 211–216, 1987.
- Ikeda K, Morizono T. Calcium transport mechanism in the endolymph of the chinchilla. *Hear Res* 34: 307–311, 1988.
- Jabba SV, Oelke A, Singh R, Maganti RJ, Fleming S, Wall SM, Everett LA, Green ED, Wangemann P. Macrophage invasion contributes to degeneration of stria vascularis in Pendred syndrome mouse model. *BMC Med* 4: 37, 2006.
- Karet FE, Finberg KE, Nelson RD, Nayir A, Mocan H, Sanjad SA, Rodriguez-Soriano J, Santos F, Cremers CW, Di Pietro A, Hoffbrand BI, Winiarski J, Bakkaloglu A, Ozen S, Dusunsel R, Goodyer P, Hulton SA, Wu DK, Skvorak AB, Morton CC, Cunningham MJ, Jha V, Lifton RP. Mutations in the gene encoding B1 subunit of H⁺-ATPase cause renal tubular acidosis with sensorineural deafness. *Nat Genet* 21: 84–90, 1999.
- Lacroix L, Mian C, Caillou B, Talbot M, Filetti S, Schlumberger M, Bidart JM. Na⁺/I⁻ symporter and Pendred syndrome gene and protein expressions in human extra-thyroidal tissues. *Eur J Endocrinol* 144: 297–302, 2001.
- Marcus DC, Rokugo M, Thalmann R. Effects of barium and ion substitutions in artificial blood on endocochlear potential. *Hear Res* 17: 79–86, 1985.
- Marcus DC, Thalmann R, Marcus NY. Respiratory quotient of stria vascularis of guinea pig in vitro. *Arch Otorhinolaryngol* 221: 97–103, 1978.
- Marcus DC, Wu T, Wangemann P, Kofuji P. KCNJ10 (Kir4.1) potassium channel knockout abolishes endocochlear potential. *Am J Physiol Cell Physiol* 282: C403–C407, 2002.
- Nakaya K, Harbidge DG, Wangemann P, Schultz BD, Green E, Wall SM, Marcus DC. Lack of pendrin HCO₃⁻ transport elevates vestibular

- endolymphatic [Ca²⁺] by inhibition of acid-sensitive TRPV5 and TRPV6 channels. *Am J Physiol Renal Physiol* 292: F1314–F1321, 2007.
25. **Ohmori H.** Mechano-electrical transduction currents in isolated vestibular hair cells of the chick. *J Physiol* 359: 189–217, 1985.
 26. **Okamura HO, Sugai N, Suzuki K, Ohtani I.** Enzyme-histochemical localization of carbonic anhydrase in the inner ear of the guinea pig and several improvements of the technique. *Histochem Cell Biol* 106: 425–430, 1996.
 27. **Oshima T, Ikeda K, Furukawa M, Takasaka T.** Alternatively spliced isoforms of the Na⁺/Ca²⁺ exchanger in the guinea pig cochlea. *Biochem Biophys Res Commun* 233: 737–741, 1997.
 28. **Pendred V.** Deaf-mutism and goitre. *Lancet* 11: 532, 1896.
 29. **Peng JB, Chen XZ, Berger UV, Vassilev PM, Brown EM, Hediger MA.** A rat kidney-specific calcium transporter in the distal nephron. *J Biol Chem* 275: 28186–28194, 2000.
 30. **Reardon W, OMahoney CF, Trembath R, Jan H, Phelps PD.** Enlarged vestibular aqueduct: a radiological marker of pendred syndrome, and mutation of the PDS gene. *QJM* 93: 99–104, 2000.
 31. **Rillema JA, Hill MA.** Prolactin regulation of the pendrin-iodide transporter in the mammary gland. *Am J Physiol Endocrinol Metab* 284: E25–E28, 2003.
 32. **Royaux IE, Suzuki K, Mori A, Katoh R, Everett LA, Kohn LD, Green ED.** Pendrin, the protein encoded by the Pendred syndrome gene (PDS), is an apical porter of iodide in the thyroid and is regulated by thyroglobulin in FRTL-5 cells. *Endocrinology* 141: 839–845, 2000.
 33. **Royaux IE, Wall SM, Karniski LP, Everett LA, Suzuki K, Knepper MA, Green ED.** Pendrin, encoded by the Pendred syndrome gene, resides in the apical region of renal intercalated cells and mediates bicarbonate secretion. *Proc Natl Acad Sci USA* 98: 4221–4226, 2001.
 34. **Scott DA, Karniski LP.** Human pendrin expressed in *Xenopus laevis* oocytes mediates chloride/formate exchange. *Am J Physiol Cell Physiol* 278: C207–C211, 2000.
 35. **Scott DA, Wang R, Kreman TM, Sheffield VC, Karniski LP.** The Pendred syndrome gene encodes a chloride-iodide transport protein. *Nat Genet* 21: 440–443, 1999.
 36. **Soleimani M, Greeley T, Petrovic S, Wang Z, Amlal H, Kopp P, Burnham CE.** Pendrin: an apical Cl⁻/OH⁻/HCO₃⁻ exchanger in the kidney cortex. *Am J Physiol Renal Physiol* 280: F356–F364, 2001.
 37. **Stankovic KM, Brown D, Alper SL, Adams JC.** Localization of pH regulating proteins H⁺ATPase and Cl⁻/HCO₃⁻ exchanger in the guinea pig inner ear. *Hear Res* 114: 21–34, 1997.
 38. **Sterkers O, Saumon G, Tran Ba Huy P, Ferrary E, Amiel C.** Electrochemical heterogeneity of the cochlear endolymph: effect of acetazolamide. *Am J Physiol Renal Fluid Electrolyte Physiol* 246: F47–F53, 1984.
 39. **Suzuki K, Royaux IE, Everett LA, Mori-Aoki A, Suzuki S, Nakamura K, Sakai T, Katoh R, Toda S, Green ED, Kohn LD.** Expression of PDS/Pds, the Pendred syndrome gene, in endometrium. *J Clin Endocrinol Metab* 87: 938–941, 2002.
 40. **Tanaka Y, Asanuma A, Yanagisawa K.** Potentials of outer hair cells and their membrane properties in cationic environments. *Hear Res* 2: 431–438, 1980.
 41. **Usami S, Abe S, Weston MD, Shinkawa H, Van Camp G, Kimberling WJ.** Non-syndromic hearing loss associated with enlarged vestibular aqueduct is caused by PDS mutations. *Hum Genet* 104: 188–192, 1999.
 42. **Vennekens R, Prenen J, Hoenderop JG, Bindels RJ, Droogmans G, Nilius B.** Modulation of the epithelial Ca²⁺ channel ECaC by extracellular pH. *Pflügers Arch* 442: 237–242, 2001.
 43. **Wangemann P.** Supporting sensory transduction: cochlear fluid homeostasis and the endocochlear potential. *J Physiol* 576: 11–21, 2006.
 44. **Wangemann P, Itza EM, Albrecht B, Wu T, Jabba SV, Maganti RJ, Lee JH, Everett LA, Wall SM, Royaux IE, Green ED, Marcus DC.** Loss of KCNJ10 protein expression abolishes endocochlear potential and causes deafness in Pendred syndrome mouse model. *BMC Med* 2: 30, 2004.
 45. **Wood JD, Muchinsky SJ, Filoteo AG, Penniston JT, Tempel BL.** Low endolymph calcium concentrations in deafwaddler2J mice suggest that PMCA2 contributes to endolymph calcium maintenance. *J Assoc Res Otolaryngol* 5: 99–110, 2004.
 46. **Yamauchi D, Raveendran NN, Pondugula SR, Kampalli SB, Sanne-man JD, Harbidge DG, Marcus DC.** Vitamin D upregulates expression of ECaC1 mRNA in semicircular canal. *Biochem Biophys Res Commun* 331: 1353–1357, 2005.
 47. **Yamoah EN, Lumpkin EA, Dumont RA, Smith PJ, Hudspeth AJ, Gillespie PG.** Plasma membrane Ca²⁺-ATPase extrudes Ca²⁺ from hair cell stereocilia. *J Neurosci* 18: 610–624, 1998.